Polymer 50 (2009) 4488–4495

Contents lists available at ScienceDirect

Polymer

journal homepage: www.elsevier.com/locate/polymer

Fabrication of hybrid nanocomposites with polystyrene and multiwalled carbon nanotubes with well-defined polystyrene via multiple atom transfer radical polymerization

Jong-Hwan Jeon, Jung-Hyurk Lim, Kyung-Min Kim*

Department of Polymer Science and Engineering, Chungju National University, Chungju, Chungbuk 380-702, Republic of Korea

ARTICLE INFO

Article history:
Received 11 May 2009
Received in revised form
8 July 2009
Accepted 21 July 2009
Available online 25 July 2009

Keywords:
Polystyrene
Multiwalled carbon nanotubes (MWNTs)
Atom transfer radical polymerization (ATRP)

ABSTRACT

The PS-grafted multiwalled carbon nanotubes (MWNTs) were produced by the bromo-ended PS (PS-Br) and pristine MWNTs in 1,2-dichlorobenzene at 110 °C for 72 h via atom transfer radical polymerization (ATRP). Bromo-ended PS (PS-Br) used as an initiator for the functionalization of MWNTs was synthesized with styrene by ATRP conditions using CuBr and N,N,N′,N′,N″-pentamethyldiethylenetriamine as catalyst. The PS-grafted MWNTs were fully characterized by ^{1}H-NMR, FT-IR, DSC, TGA, and SEM. The PS-grafted MWNTs were found to be highly soluble in a variety of organic solvents. The PS was chemically attached to the surfaces of MWNTs via ATRP approach, and the grafting amount of PS was 40–90%. From TGA and DSC measurements, the PS-grafted MWNTs were decomposed at lower temperature compared to that of PS-Br, and the functionalization of MWNTs increased the glass-transition temperature (T_g) of the grafted PS. The PS/PS-grafted MWNTs nanocomposites were prepared with PS and PS-grafted MWNTs by solution mixing in dimethylformamide (DMF). The resulting nanocomposites were found to be the homogeneous dispersion of PS-grafted MWNTs in PS matrix via aromatic (π–π) interactions between PS and PS-grafted MWNTs as determined by SEM and TEM.

1. Introduction

It is well-known that carbon nanotubes (CNTs) have outstanding mechanical and electrical properties, which provide potential in nanotechnology and electronic nanodevices [1,2]. Recently, polymer/CNTs composites have attracted considerable attention because the individual properties of the two components can be combined to give novel hybrid nanomaterials with good mechanical strength, unique multifunctional properties, and excellent processability [3,4]. However, despite excellent properties of polymer/CNTs composites as mentioned above, the poor solubility and self-aggregation of CNTs with strong van der Waals forces disturb the improved properties of polymer/CNTs composites, which has been still remaining as a challenge for both academia and industry [5]. Therefore, the major issues for preparing the polymer/CNTs composites are the homogeneous dispersion and interfacial compatibility with the polymer matrix without agglomeration and exfoliation of CNTs bundles.

Thus, many research groups have focused on the functionalization of CNTs with various organic, inorganic, and organometallic structures using both non-covalent and covalent approaches [6]. Non-covalent interactions such as π–π interactions, π–cation interactions, and ionic interactions between CNTs and polymers enable the attachment of polymers onto the surfaces of CNTs [7–11]. The covalent functionalization of CNTs with polymers includes effective both "grafting-from" and "grafting-to" approaches. For the "grafting-from" method, polymers are in-situ grown from CNTs commonly using surface-initiated polymerization such as atom transfer radical polymerization (ATRP) [12–19], and reversible addition–fragmentation chain transfer polymerization [20,21]. For the "grafting-to" method, preformed polymers are grafted to CNTs through special reactions such as esterification and amidization between suitable functional groups of CNTs and polymers [22–25].

In the present report, we describe the use of ATRP to prepare well-defined, narrow polydispersity polystyrene (PS), followed by its attachment to the surfaces of multiwalled carbon nanotubes (MWNTs) using ATRP one more time. That is, PS-grafted MWNTs were synthesized by the reaction of bromo-ended PS (PS-Br) and purified MWNTs using the novel "grafting-to" approach via ATRP two times, by which method PS-Br synthesized by ATRP was allowed to react directly with MWNTs in 1,2-dichlorobenzene under ATRP conditions using CuBr and N,N,N′,N′,N″-pentamethyldiethylenetriamine as catalyst system. In the general "grafting-to" method, some defects are that low polymer loadings onto

* Corresponding author. Tel.: +82 43 841 5429; fax: +82 43 841 5420.
E-mail address: kmkim@chungju.ac.kr (K.-M. Kim).

0032-3861/$ – see front matter © 2009 Elsevier Ltd. All rights reserved.
doi:10.1016/j.polymer.2009.07.033

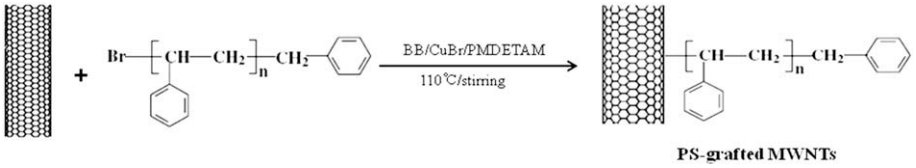

Scheme 1. Synthesis of PS-grafted MWNTs.

the surfaces of CNTs are possible due to a steric repulsion between grafted and reacting polymer chain, and practical application of CNTs suffers from the poor solubility caused by a low degree of surface functionalization. In addition, several synthetic steps to make MWNTs-supported initiator for in-situ polymerization of various monomers must be needed in the normal "grafting-from" method, by which characterization of the incorporated polymer on the MWNTs is impossible. To address some problems derived from both normal "grafting-from" and "grafting-to" approaches, our new "grafting-to" approach for PS-grafted MWNTs was favored because it allows for the higher degree of the grafted polymer chains and clear characterization of polymer structure before the grafting step. Furthermore, this novel approach makes it easier to achieve our final goal which is homogeneous dispersion of PS-grafted MWNTs in PS matrix.

To the best of our knowledge, there is no report in the literature regarding the use of well-defined PS-Br obtained by ATRP as an initiator instead of MWNTs-supported initiator and its grafting to the convex walls of MWNTs by ATRP one more time. The obtained PS-grafted MWNTs showed that PS was chemically grafted onto the surfaces of MWNTs, and the grafting amount of PS was 40–90% from TGA results. This extremely high grafting efficiency is surprising because several reports dealing with the functionalization of CNTs using normal "grafting-to" approach show that the maximum grafting amount of polymer is around 8–48% [26,27]. The resulting PS-grafted MWNTs exhibit a high solubility in various organic solvents except water, which indicate that well-defined PS is successfully attached to the surfaces of MWNTs. The higher incorporation of PS onto the MWNTs and good solubility of PS-grafted MWNTs using the novel "grafting-to" approach is necessary for the homogeneous hybrid nanocomposites with PS and PS-grafted MWNTs. The PS/PS-grafted MWNTs hybrid nanocomposites are prepared by solution mixing of PS and PS-grafted MWNTs in DMF. For the composites containing PS and pristine MWNTs, several aggregated masses of MWNTs are easily observed on the morphology, whereas PS-grafted MWNTs are spatially well dispersed in PS matrix through aromatic (π–π) interactions between PS and PS-grafted MWNTs.

2. Experimental section

2.1. Materials

Pristine MWNTs were obtained from the Iljin Nanotech Inc. (diameter: 10–20 nm, length: 10–50 μm, >90 vol% of purity). Polycarbonate membrane (pore size: 200 nm) was obtained from the Whatman International Ltd. Styrene was dried over CaH_2, and distilled under vacuum. Benzyl bromide (BB) was distilled before use. Copper (II) bromide (CuBr) was washed subsequently by acetic acid and ethanol and then dried under vacuum. 1,2-Dichlorobenzene (DCB) was distilled over CaH_2 under vacuum. Tetrahydrofuran (THF) was distilled from $LiAlH_4$ under nitrogen. N,N,N′,N′,N″-pentamethyldiethylenetriamine (PMDETAM), methanol, and nitric acid (HNO_3) were purchased from Aldrich.

2.2. Measurements

^{1}H-NMR spectra were obtained on a 400 MHz AVANVE 400FT-NMR (BRUKER) spectrometer. Fourier transform infrared (FT-IR) spectra were recorded on a FTS-6000 (BIO-RAD) spectrometer. The thermal behavior was examined with differential scanning calorimetry (DSC) (DSC 2010, TA Instruments) and thermogravimetric analysis (TGA) (TGA S-1000, SCINCO) under nitrogen atmospheres, respectively. Raman spectrophotometer (NRS-3200, JASCO) was used to confirm and characterize PS-grafted MWNTs which was formed after the modification of pristine MWNTs under ATRP condition. The morphologies and structures of PS/PS-grafted MWNTs nanocomposites were observed by scanning electron microscopy (SEM) (JSM-6700, JEOL) and Energy Filtering Transmission Electron Microscope (EF-TEM) (Libra 120, ZEISS). For EF-TEM observation,

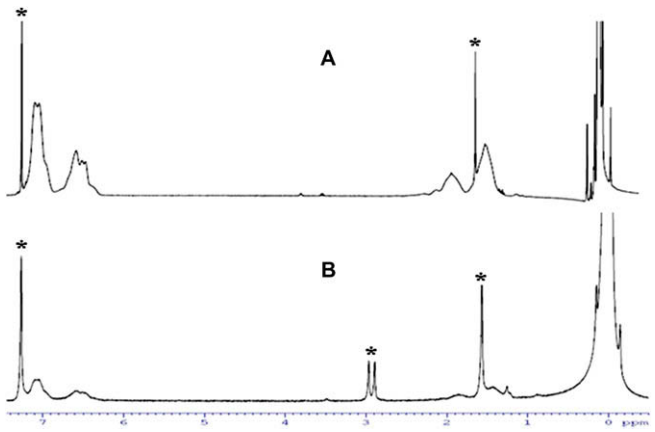

Fig. 1. ^{1}H-NMR (400 MHz) spectra of (A) PS-Br and (B) PS-grafted MWNTs in $CDCl_3$. Asterisks show the peak due to solvents.

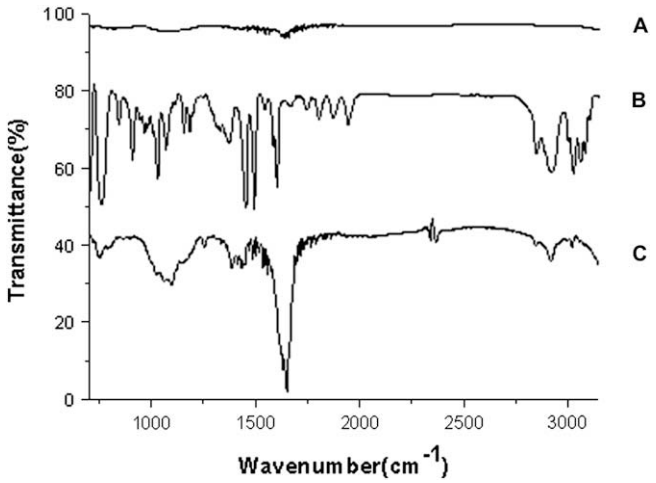

Fig. 2. FT-IR spectra of (A) pristine MWNTs, (B) PS-Br, and (C) PS-grafted MWNTs with KBr.

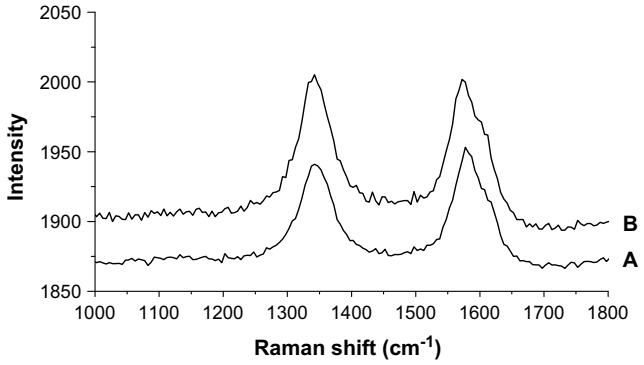

Fig. 3. Raman spectra of pristine MWNTs (A) and PS-grafted MWNTs (B).

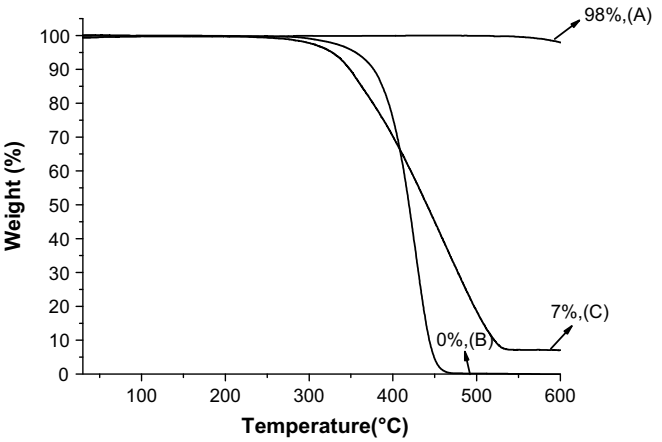

Fig. 5. TGA thermograms of (A) pristine MWNTs, (B) PS-Br, and (C) PS-grafted MWNTs with a heating rate of 10 °C/min under nitrogen atmosphere.

PS/PS-grafted MWNTs nanocomposites were redissolved in chloroform and the solution was dropped onto a copper grid and then dried under vacuum. Polymer molecular weight and polydispersity index (PDI) were estimated by gel permeation chromatography (GPC) using an Agilent Technologies 1200 series. Polystyrene standards were used for calibration, and tetrahydrofuran (THF) was used as the eluent at a flow rate of 1.0 mL/min.

2.3. Purification of MWNTs

Multiwalled carbon nanotubes (MWNTs) were heated and refluxed in 100 mL of 60% HNO_3 aqueous solution for 3 h. After cooling to room temperature, it was diluted with 400 mL of deionized water and then vacuum filtered through a 200 nm polycarbonate membrane. The solid was washed with deionized water until neutral pH value, and then dried under vacuum.

2.4. Synthesis of bromo-ended polystyrene (PS-Br)

A 50 mL round-bottom flask was charged with benzyl bromide (0.31 g, 1.8 mmol), CuBr (0.40 g, 1.8 mmol), and N,N,N′,N′,N″-pentamethyldiethylenetriamine (0.94 g, 5.4 mmol). Then the solution was sealed with a rubber septum. After the mixture was degassed three times, the monomer styrene (20.0 g, 0.19 mol) was added using flamed syringe. The mixture was charged under dry nitrogen for 30 min and the flask was placed into a 110 °C oil bath. The reaction was allowed to proceed for 12 h, and the reaction mixture was dissolved in THF and then precipitated by dropwise addition of the solution into methanol. The precipitate was redissolved in THF and the solution was filtered through a neutral alumina column to remove the catalyst. The polymer was recovered by precipitation with a large excess of methanol and dried under vacuum. The product was analyzed by GPC ($M_n = 11{,}000$ g/mol, PDI = 1.33). ^{1}H-NMR (400 MHz, $CDCl_3$): δ 7.06 (broad), 6.50 (broad), 1.86 (broad), and 1.43 ppm (broad).

2.5. Synthesis of PS-grafted MWNTs

0.5 g of purified MWNTs and 50 mL of 1,2-dichlorobenzene were introduced into a 250 mL flask, and the mixture was sonicated for 30 min. Then PS-Br (12.0 g), CuBr (0.22 g, 0.99 mmol), N,N,N′,N′,N″-pentamethyldiethylenetriamine (0.67 g, 3.9 mmol), and 100 mL of 1,2-dichlorobenzene were charged. After stirring 2 h at room temperature to form a black suspension, the glass was fitted with a condenser and the mixture was stirred at 110 °C under nitrogen for 72 h. After cooling to room temperature, the reaction mixture was diluted with 200 mL of 1,2-dichlorobenzene, and then the mixture was sonicated for 40 min. The mixture was collected by filtering through a 200 nm pore polycarbonate membrane while washing thoroughly with 1,2-dichlorobenzene and methanol, and then the purified product was dried under vacuum overnight.

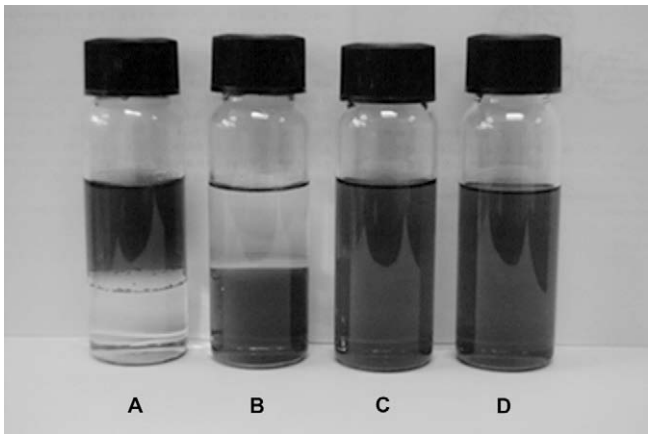

Fig. 4. Solutions of MWNTs samples in various solvents: (A) purified MWNTs in CH_2Cl_2/H_2O; (B) PS-grafted MWNTs in CH_2Cl_2/H_2O; (C) PS-grafted MWNTs in THF; (D) PS-grafted MWNTs in $CHCl_3$.

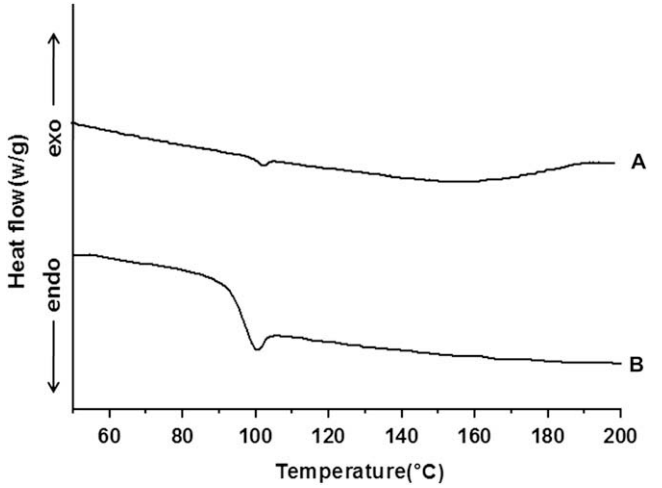

Fig. 6. DSC thermograms of (A) PS-grafted MWNTs and (B) PS-Br with a heating rate of 10 °C/min under nitrogen atmosphere.

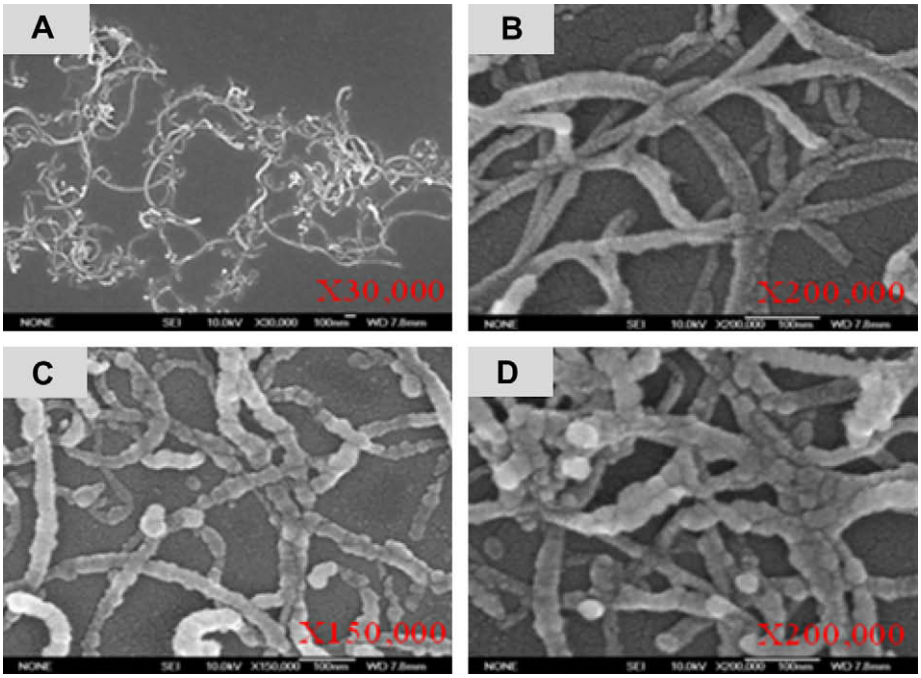

Fig. 7. FE-SEM images of (A, B) pristine MWNTs and (C, D) PS-grafted MWNTs on Si-wafer.

The ^{1}H-NMR (400 MHz, $CDCl_3$): δ 7.08 (broad), 6.52 (broad), 1.83 (broad), and 1.45 ppm (broad). The content of grafted PS onto the surfaces of MWNTs was 40–90% as determined by TGA.

2.6. Fabrication of hybrid PS/PS-grafted MWNTs nanocomposites

The PS/PS-grafted MWNTs nanocomposites were prepared by solution mixing in DMF. 6.0 mg of PS-grafted MWNTs and 20 mL of DMF were added into a 50 mL flask and sonicated for 2 h at room temperature to obtain homogeneous solution. Then 6.0 g of PS was added into the solution. The mixture was further stirred for 1 h and sonicated for 1 h, and then precipitated by dropwise addition of the solution into methanol. The precipitate was filtered through a 200 nm pore membrane and dried under vacuum. (PS/pristine MWNTs composites were prepared by same procedures used for PS/PS-grafted MWNTs nanocomposites).

3. Results and discussion

To prepare PS-grafted MWNTs with PS that is more densely grafted, well-defined PS-Br as an initiator was prepared by well-known ATRP which is one of the most promising polymerization approaches to control molecular weight and its distribution within the resulting polymers [28,29]. The PS-Br having a molecular weight of 11,000 g/mol and a polydispersity of 1.33 was obtained. The PS-grafted MWNTs were synthesized by PS-Br and MWNTs via ATRP process (Scheme 1). That is, our new approach, novel "grafting-to" method contains multiple ATRP process (two times) for the functionalization of MWNTs. The advantages of our novel approach are that high polymer loading onto the surfaces of MWNTs and good solubility of polymer-grafted MWNTs resulted in the homogeneous dispersion of MWNTs in polymer matrix which is still difficult problem to solve so far.

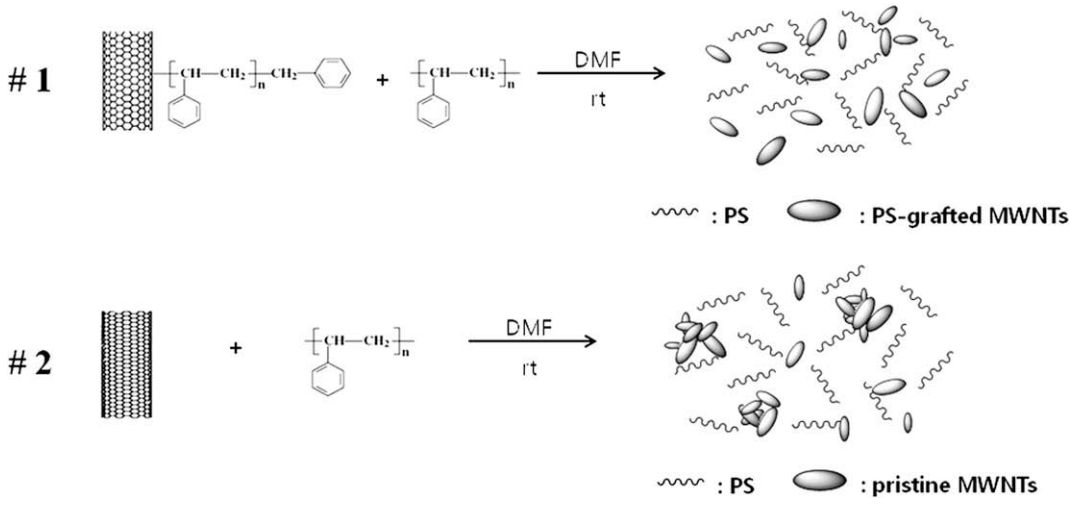

Scheme 2. Fabrication of PS/PS-grafted MWNTs nanocomposites and PS/pristine MWNTs composites, respectively, by solution mixing.

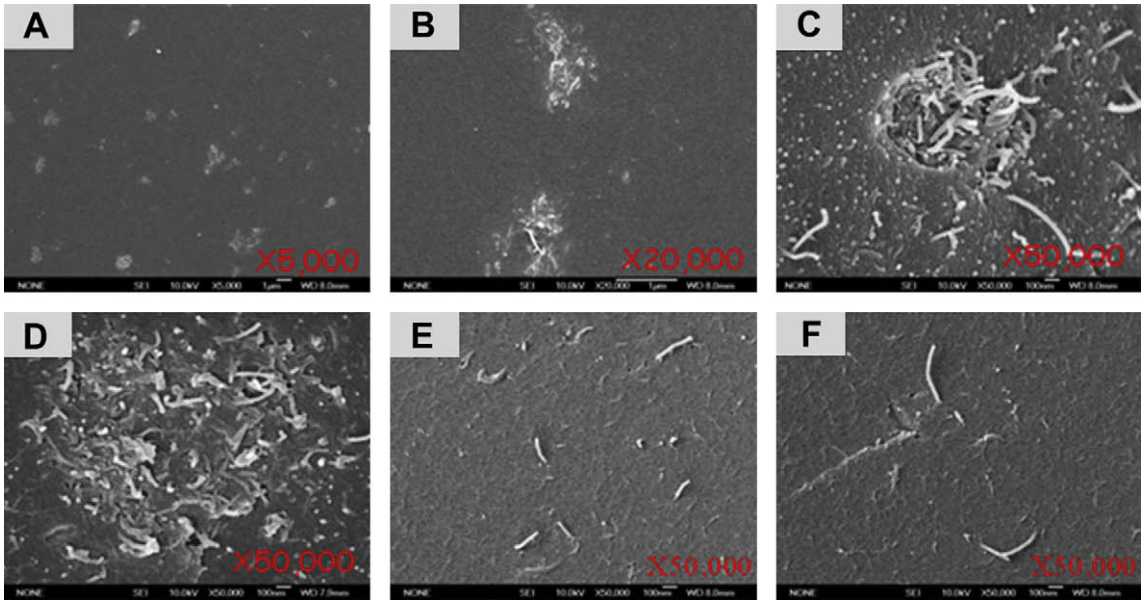

Fig. 8. FE-SEM images of (A–D) PS/pristine MWNTs composites and (E, F) PS/PS-grafted MWNTs nanocomposites on Si-wafer.

Fig. 1 depicts the ^{1}H-NMR spectra of PS-Br used an initiator for the functionalization of MWNTs and PS-grafted MWNTs. Two spectra are nearly identical, clearly illustrating that PS was attached to the external walls of MWNTs. Both of the spectra show the expected aromatic signals for PS at 7.06 and 6.50 ppm as well as the backbone signals at 1.86 and 1.43 ppm.

Fig. 2 presents the FT-IR spectra of pristine MWNTs, PS-Br, and PS-grafted MWNTs. The spectrum of pristine MWNTs shows a weak absorption peak at 1632 cm^{-1}, which is related to the C=C stretching vibration of MWNTs backbones. The spectrum of PS-Br shows CH stretching peak of the aromatic ring at 3020 cm^{-1}, CH asymmetric stretching peak of the CH_2 group at 2920 cm^{-1}, C=C stretching vibration of the aromatic ring at 1600–1440 cm^{-1}, and mono-substitute at 690–760 cm^{-1}. After surface modification of MWNTs, new absorption peak for aromatic ring in the region of 1600–1440 cm^{-1} occurred as a result of grafted PS onto the surfaces of MWNTs. As shown in Fig. 2C, for PS-grafted MWNTs, there appeared three new peaks at 1600, 1490, and 1448 cm^{-1} that are all characteristic of PS-Br and are not seen in the spectrum of pristine MWNTs.

Raman spectroscopy provides qualitative information about the polymer-modified MWNTs. Raman spectra of pristine MWNTs and

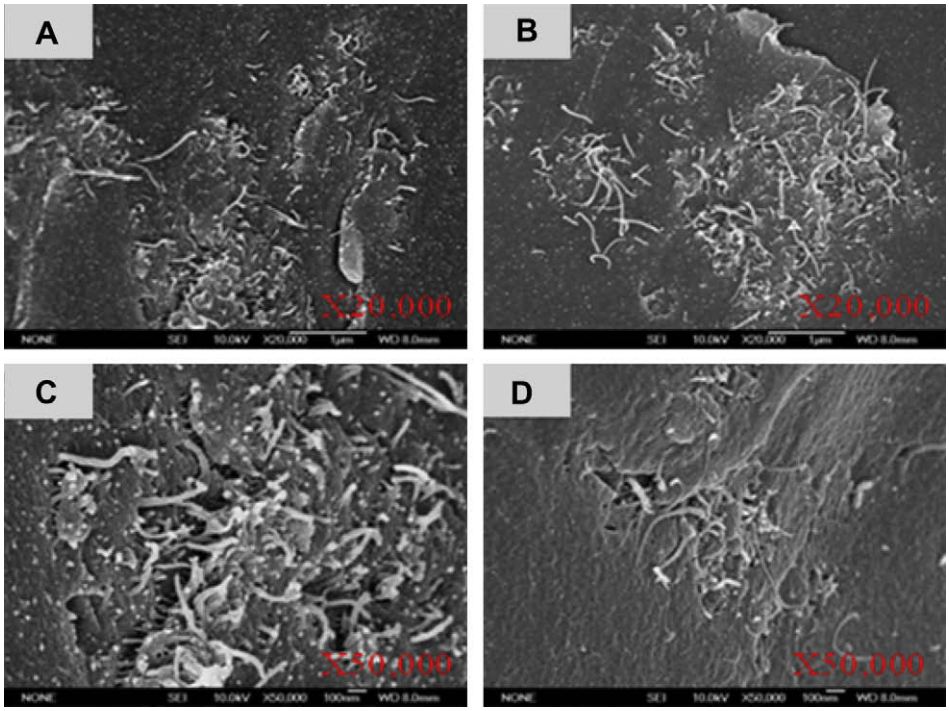

Fig. 9. FE-SEM images of cryogenically fractured surfaces of PS/pristine MWNTs composites on Si-wafer.

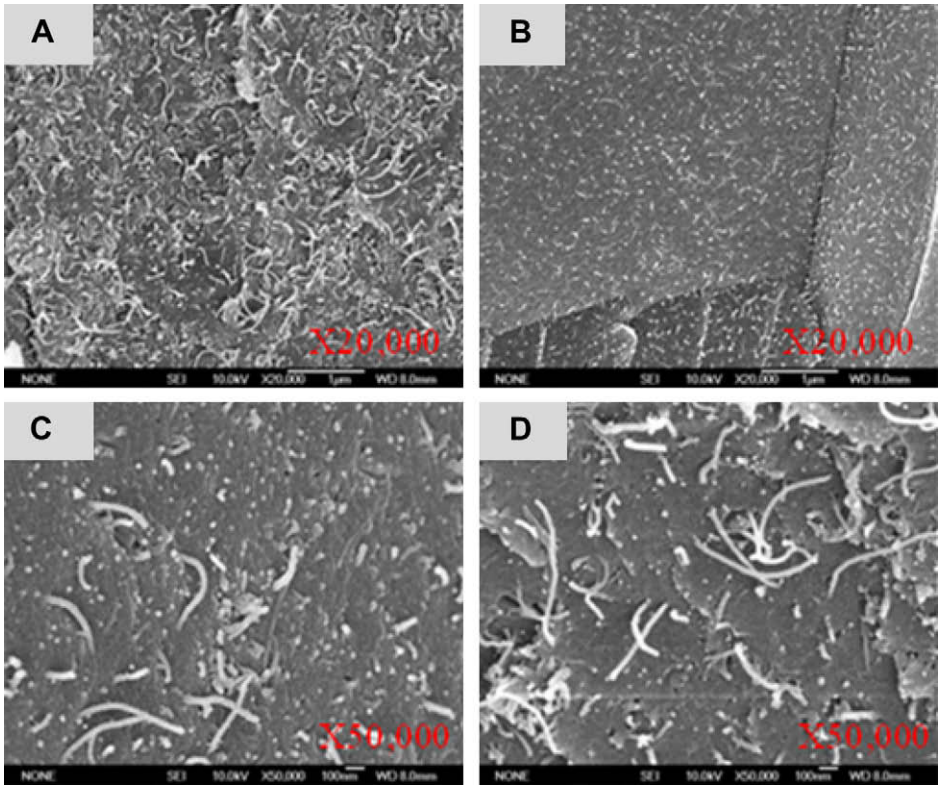

Fig. 10. FE-SEM images of cryogenically fractured surfaces of PS/PS-grafted MWNTs nanocomposites on Si-wafer.

PS-grafted MWNTs display two obvious peaks as shown in Fig. 3. This shows characteristic G-mode or the tangential mode peaks at 1580 cm^{-1} and a disorder transition D band peaks at 1345 cm^{-1} for pristine and PS-grafted MWNTs, respectively. In general, the intensity of the D band is used to probe the degree of modification. Fig. 3B shows that the intensity enhancement of D band in PS-grafted MWNTs proves the covalent bonding of PS onto the MWNTs. The ratio of the intensity of the disordered (D band) to the ordered (G band) transition, which indicates the generation of surface defects due to modification, increases from 0.97 (pristine MWNTs) to 1.01 (PS-grafted MWNTs).

It was found that the functionalization of MWNTs drastically affected the solubility characteristics of purified MWNTs and PS-grafted MWNTs. Fig. 4 shows the solubility of purified MWNTs and PS-grafted MWNTs in the water and various organic solvents. For each experiment, the concentration of MWNTs and PS-grafted MWNTs in the solvents was 1 mg/mL. The resulting mixture was ultrasonicated by using a bath-type ultrasonicator for 8 h. As illustrated in Fig. 4A, the initial purified MWNTs exhibit solubility in water before the functionalization of PS. However, after functionalization with PS-Br via ATRP, PS-grafted MWNTs lost its solubility in H_2O and became highly soluble in organic solvents, including CH_2Cl_2, THF, and $CHCl_3$ (Fig. 4B–D). The appearance of solubility change and high solubility made us to confirm that well-defined PS-Br was effectively grafted to MWNTs via ATRP.

The relative amounts of grafted PS and MWNTs were determined by TGA through the thermal decomposition of PS, because PS had a lower decomposition temperature than MWNTs. Fig. 5 shows TGA traces of pristine MWNTs, PS-Br, and PS-grafted MWNTs in an inert atmosphere at a heating rate of 10 °C/min. Clearly, pristine MWNTs have good thermal stability. When the temperature is increased up to 600 °C, there is no obvious decomposition in pristine MWNTs. The PS-Br completely decomposes in the temperature range between 355 and 460 °C. The weight of PS-grafted MWNTs rapidly decreased near 320 °C, because of the decomposition of PS, leaving residual MWNTs at temperature higher than 600 °C. Neat MWNTs hardly decomposed at temperature below 600 °C. Therefore, the TGA results can be applied to estimate the relative amounts of the grafted PS onto the convex walls of MWNTs. The difference in the weight loss at 600 °C between PS-grafted MWNTs and pristine MWNTs showed that the PS grafting amount is about 40–90%. This higher well-defined PS loading onto the surfaces of MWNTs through multiple ATRP is amazing as compared to the previously reported literatures [26,27]. Unexpectedly, the initial decomposition temperature of PS-grafted MWNTs was lower than that of PS-Br. This result is possibly due to the high thermal conductivity of MWNTs in the PS-grafted MWNTs [30].

Fig. 6 shows the DSC curves of PS-Br and PS-grafted MWNTs. The glass-transition temperature (T_g) of the PS chains in PS-grafted MWNTs shifts to a higher temperature (103 °C) than that of PS-Br (98 °C). The reason is that the covalent incorporation of PS to the surfaces of MWNTs via ATRP approach restricts the segmental motions of PS chain.

As described above, all the characterizations effectively demonstrate that the well-defined PS chains are covalently grafted onto the MWNTs with high loading efficiency via ATRP. Measurements of SEM images can provide further direct evidence for PS-grafted MWNTs. Thus, SEM images of the pristine MWNTs and PS-grafted MWNTs are shown in Fig. 7. Fig. 7A and B presents typical SEM images of the pristine MWNTs, showing a very clean surface for all the MWNTs. However, the functionalization of MWNTs with PS-Br significantly alters the surface roughness of the MWNTs surface, with a significant increase in the diameter of the MWNTs. In addition, irregular structures observed on the MWNTs surface reveal that the functionalization takes place in spherical shapes present on the MWNTs surface as shown in Fig. 7C and D.

In general, MWNTs can easily aggregate each other due to the high surface area and van der Waals attraction, which still faces the

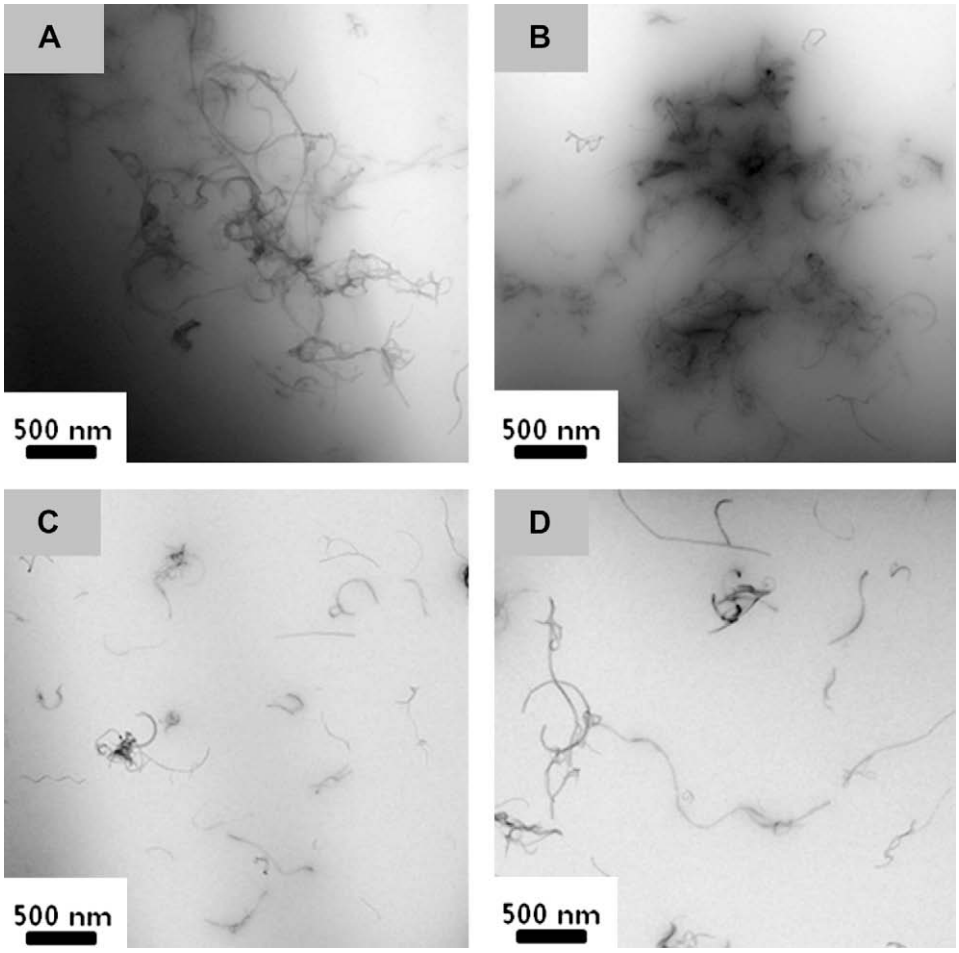

Fig. 11. TEM images of (A, B) PS/pristine MWNTs composites and (C, D) PS/PS-grafted MWNTs nanocomposites.

problem of good dispersion. To overcome this disadvantage, PS-grafted MWNTs using the novel "grafting-to" approach via multiple ATRP method were applied to fabricate the homogeneous hybrid nanocomposites. The PS/PS-grafted MWNTs nanocomposites were prepared with PS and PS-grafted MWNTs by solution mixing in DMF. The PS (10 g) and PS-grafted MWNTs (0.01 g) were dissolved in 20 mL of DMF (Scheme 2). The solution was then dropped on Si-wafer and the solvent was allowed to evaporate slowly. The nanocomposite film was then dried in a vacuum oven at 50 °C for 48 h. The PS/pristine MWNTs composites for a control experiment were prepared by same procedures used in PS/PS-grafted MWNTs nanocomposites.

Fig. 8 shows the SEM microphotographs of PS/pristine MWNTs composites and PS/PS-grafted MWNTs nanocomposites where 0.1 wt% of pristine MWNTs and PS-grafted MWNTs are incorporated, respectively. For the composites containing pristine MWNTs, severely aggregated masses of MWNTs are frequently observed on the morphology as seen in Fig. 8A–D, whereas in case of PS/PS-grafted MWNTs nanocomposites, PS-grafted MWNTs are spatially well dispersed in the PS matrix as shown in Fig. 8E and F. Pristine MWNTs were aggregated each other because there is no interaction between pristine MWNTs and PS. The homogeneous dispersion of PS-grafted MWNTs is ascribed to the aromatic (π–π) interactions between phenyl groups of PS and PS-grafted MWNTs. The effectiveness of aromatic (π–π) interactions was already supported and verified by our reported literatures [31–33]. The much improved dispersion of PS-grafted MWNTs in the PS matrix well corresponds to the result investigated by SEM microphotographs of cryogenically fractured surfaces of PS/pristine MWNTs composites and PS/PS-grafted MWNTs nanocomposites as shown in Figs. 9 and 10, respectively. Pristine MWNTs were lumped in the PS matrix as shown in Fig. 9, whereas PS-grafted MWNTs were nicely, homogeneously dispersed in the PS matrix through aromatic (π–π) interactions between phenyl groups of PS and PS-grafted MWNTs as shown in Fig. 10. We have found that the formation of well dispersed PS/PS-grafted MWNTs nanocomposites can be achieved by the surface modification of MWNTs with well-defined PS via ATRP approach.

For TEM observation, the samples of PS/PS-grafted MWNTs nanocomposites were prepared by redissolving in chloroform and the solution was dropped onto a copper grid and then dried under vacuum. The morphology of PS/pristine MWNTs composites and PS/PS-grafted MWNTs nanocomposites was characterized by TEM. From the result of TEM measurement of PS/pristine MWNTs composites and PS/PS-grafted MWNTs nanocomposites, we clearly confirmed that PS-grafted MWNTs were homogeneously dispersed in PS matrix via aromatic interactions as the same results of SEM. For the composites containing pristine MWNTs, aggregated masses of MWNTs are observed in the PS matrix as seen in Fig. 11A and B, whereas PS-grafted MWNTs are spatially well dispersed in the PS matrix as shown in Fig. 11C and D.

4. Conclusions

ATRP approach was used to prepare well-defined PS which was covalently attached to MWNTs by using ATRP method one more time in the presence of MWNTs, which led to PS-grafted MWNTs with an efficient loading of PS to MWNTs sidewalls. The resulting

PS-grafted MWNTs were highly soluble in various organic solvents and the grafting amount of PS to MWNTs sidewalls was 40–90%. The glass-transition temperature (T_g) of PS-grafted MWNTs was higher than that of PS-Br, indicating that MWNTs disturbed the segmental motions of the grafted PS. This new approach, what is called, "grafting-to" method could settle the disadvantages derived from the existing both "grafting-from" and "grafting-to" approaches. Furthermore, the PS/PS-grafted MWNTs nanocomposites were prepared by PS-grafted MWNTs with excellent properties and PS in DMF solution to solve the dispersion problem of MWNTs. The PS-grafted MWNTs were homogeneously dispersed in PS matrix via aromatic (π–π) interactions between phenyl groups of PS and PS-grafted MWNTs, which was clearly observed in SEM and TEM images. In this hybrid system, aromatic (π–π) interactions played a critical role in the formation of the homogeneous hybrid nanocomposites with PS and PS-grafted MWNTs.

Acknowledgement

This work was supported by the Korean Research Foundation Grant funded by the Korean Government (MOEHRD) (KRF-2008-041-D00233) and the Program for the Training of Graduate Students in Regional Innovation conducted by the Ministry of Commerce, Industry and Energy of the Korean Government.

References

[1] Baughman RH, Zakhidov AA, Deheer WA. Science 2002;297:787.
[2] Ajayan PM. Chem Rev 1999;99:1787.
[3] Shaffer MSP, Windle AH. Adv Mater 1999;11:937.
[4] Haggenmueller R, Gommans HH, Rinzler AG, Fischer JE, Winey KI. Chem Phys Lett 2000;330:219.
[5] Park C, Oundaies Z, Watson KA, Crooks RE, Smith JJ, Lowther SE, et al. Chem Phys Lett 2002;364:303.
[6] Hirsch A. Angew Chem Int Ed 2002;41:1853.
[7] Kim KH, Jo WH. Macromolecules 2007;40:3708.
[8] Lee JU, Huh J, Kim KH, Park C, Jo WH. Carbon 2007;45:1051.
[9] Wang M, Pramoda KP, Goh SH. Carbon 2006;44:613.
[10] Park S, Huh JO, Kim NG, Kang SM, Lee KB, Hong SP. Carbon 2008;46:706.
[11] Xue CH, Zhou RJ, Shi MM, Gao Y, Wu G, Zhang ZB. Nanotechnology 2008;19:215604.
[12] Shanmugharaj AM, Bae JH, Nayak RR, Ryu SH. J Polym Sci Part A Polym Chem 2007;45:460.
[13] Qin S, Qin D, Ford WT, Resasco DE, Herrera JE. J Am Chem Soc 2004;126:170.
[14] Kong H, Gao C, Yan D. J Am Chem Soc 2004;126:412.
[15] Kong H, Gao C, Yan D. Macromolecules 2004;37:4022.
[16] Qin S, Qin D, Ford WT, Resasco DE, Herrera JE. Macromolecules 2004;37:752.
[17] Baskaran D, Mays JW, Bratcher MS. Angew Chem Int Ed 2004;43:2138.
[18] Hong CY, You YZ, Wu DC, Liu Y, Pan CY. Macromolecules 2005;38:2606.
[19] Liu YL, Chen WH. Macromolecules 2007;40:8881.
[20] You YZ, Hong CY, Pan CY. Nanotechnology 2006;17:2350.
[21] Hong CY, You YZ, Pan CY. Polymer 2006;47:4300.
[22] Zhao B, Hu H, Yu A, Perea D, Haddon RC. J Am Chem Soc 2005;127:8197.
[23] Li H, Cheng F, Duft AM, Adronov A. J Am Chem Soc 2005;127:14518.
[24] Hill D, Lin Y, Qu L, Kitaygorodskiy A, Connell JW, Allard LF. Macromolecules 2005;38:7670.
[25] Wang W, Lin Y, Sun YP. Polymer 2005;46:8634.
[26] Nayak RR, Lee KY, Shanmugharaj AM, Ryu SH. Eur Polym J 2007;43:4916.
[27] Zhao W, Liu YT, Feng QP, Xie XM, Wang XH, Ye XY. J Appl Polym Sci 2008;109:3525.
[28] Wang JS, Matyjaszewski KJ. J Am Chem Soc 1995;117:5614.
[29] Matyjaszewski KJ, Xia J. Chem Rev 2001;101:2921.
[30] Liu Y, Yao Z, Adronov A. Macromolecules 2005;38:1172.
[31] Tamaki R, Han S, Chujo Y. Silicon Chemistry 2002;1:409.
[32] Kim KM. Polymer (Korea) 2006;30:380.
[33] Kim KM, Ogoshi T, Chujo Y. J Polym Sci Part A Polym Chem 2005;43:473.